© 2015. Published by The Company of Biologists Ltd | The Journal of Experimental Biology (2015) 218, 370-380 doi:10.1242/jeb.114942

RESEARCH ARTICLE

Comparative structural and functional analysis of the larval and adult dorsal vessel and its role in hemolymph circulation in the mosquito *Anopheles gambiae*

Garrett P. League, Ogechukwu C. Onuh and Julián F. Hillyer*

ABSTRACT

Hemolymph circulation in insects is driven primarily by the contractile action of a dorsal vessel, which is divided into an abdominal heart and a thoracic aorta. As holometabolous insects, mosquitoes undergo striking morphological and physiological changes during metamorphosis. This study presents a comprehensive structural and functional analysis of the larval and adult dorsal vessel in the malaria mosquito *Anopheles gambiae*. Using intravital video imaging we show that, unlike the adult heart, the larval heart contracts exclusively in the anterograde direction and does not undergo heartbeat directional reversals. The larval heart contracts 24% slower than the adult heart, and hemolymph travels across the larval dorsal vessel at a velocity that is 68% slower than what is seen in adults. By fluorescently labeling muscle tissue we show that although the general structure of the heart and its ostia are similar across life stages, the heart-associated alary muscles are significantly less robust in larvae. Furthermore, unlike the adult ostia, which are the entry points for hemolymph into the heart, the larval ostia are almost entirely lacking in incurrent function. Instead, hemolymph enters the larval heart through incurrent openings located at the posterior terminus of the heart. These posterior openings are structurally similar across life stages, but in adults have an opposite, excurrent function. Finally, the larval aorta and heart differ significantly in the arrangement of their cardiomyocytes. In summary, this study provides an in-depth developmental comparison of the circulatory system of larval and adult mosquitoes.

KEY WORDS: Heart, Contraction, Aorta, Hemocoel, Larva, Diptera

INTRODUCTION

Circulation of hemolymph (blood) in the insect open circulatory system is essential for the transport of nutrients, waste, signalling molecules and immune factors throughout the hemocoel (body cavity) (Chapman et al., 2013; Klowden, 2013). Hemolymph circulation is accomplished primarily via the pumping action of a muscular dorsal vessel that lies beneath the dorsal cuticle and runs the length of the body along the dorsal midline. The dorsal vessel consists of two distinct regions: the abdominal heart and the thoracic aorta. The heart is a pulsatile organ that contains ostia (valves) that allow hemolymph to enter the lumen of the vessel, whereas the aorta serves as a passive conduit for hemolymph propelled into the thorax by the contractile action of the heart.

In adult mosquitoes, intravital imaging has revealed that the heart contracts bidirectionally, propelling hemolymph towards the head (anterograde) and towards the posterior of the abdomen (retrograde) (Andereck et al., 2010; Glenn et al., 2010). During anterograde heart contractions, hemolymph enters the lumen of the dorsal vessel via incurrent ostia located at the anterior portion of abdominal segments 2–7 and exits into the head via an excurrent opening located at the anterior end of the aorta. During retrograde heart contractions, however, hemolymph enters the dorsal vessel via a single pair of ostia located at the thoraco-abdominal junction and exits into the abdominal hemocoel via a pair of excurrent openings located at the posterior terminus of the heart (Glenn et al., 2010).

Studies on heart function and hemolymph flow dynamics in anopheline mosquitoes have yielded important insights into both immunity (King and Hillyer, 2012) and circulation (Andereck et al., 2010; Glenn et al., 2010; Estévez-Lao et al., 2013; Boppana and Hillyer, 2014). However, these studies in *Anopheles gambiae* have focused on the adult life stage without addressing how hemolymph is propelled in the immature stages. As holometabolous insects, mosquitoes undergo dramatic changes en route to adulthood. Mosquitoes lay their eggs in water, where they hatch into larvae, develop through four larval instars, pupate and, finally, emerge into terrestrial environments as airborne adults. Because larvae are adapted to swimming and feeding in aquatic habitats and have yet to undergo the metamorphic changes necessary for flight and reproduction, the larval body plan differs significantly from that of adults. A recent study in the distantly related culicine mosquito, *Aedes aegypti*, compared the ultrastructure of the larval, pupal and adult heart, and found that the structure and arrangement of the cardiomyocytes is similar across all life stages, with major differences occurring primarily in heart-associated tissues such as the alary muscles (Leódido et al., 2013). However, no mosquito study on the larval stage has coupled structural data on the dorsal vessel with functional data on hemolymph flow. The only study that has ventured into a related area used brightfield light microscopy to compare, at a gross level, larval and adult dorsal vessel structure and heart contractions, but this study did not visualize hemolymph flow or flow mechanics (Jones, 1954).

Although little attention has been given to larval circulation and heart structure in mosquitoes, larval studies in the fellow dipteran *Drosophila melanogaster* have increased our understanding of cardiac function in immature insects while also serving as a model for human cardiac physiology (Curtis et al., 1999; Molina and Cripps, 2001; Sláma and Farkas, 2005; Babcock et al., 2008; Piazza and Wessells, 2011; Lehmacher et al., 2012). Furthermore, as the insect heart and associated tissues are restructured or even destroyed during the pupa to adult transition (Smits et al., 2000; Molina and Cripps, 2001; Lehmacher et al., 2012; King and Hillyer, 2013; Leódido et al., 2013), larval heart structure and circulatory dynamics cannot merely be inferred from observations in adults. Here, we used live imaging techniques to visualize and quantify heart

Department of Biological Sciences, Vanderbilt University, Nashville, TN 37235, USA.

*Author for correspondence (julian.hillyer@vanderbilt.edu)

Received 1 October 2014; Accepted 1 December 2014

The Journal of Experimental Biology

The Journal of Experimental Biology (2015) doi:10.1242/jeb.114942

contraction dynamics and hemolymph flow velocity in *A. gambiae* fourth instar larvae and adults. We show that the larval heart contracts exclusively in the anterograde direction, and that heart contraction rates and hemolymph flow velocity are slower in larvae when compared with adults. Furthermore, we present a comprehensive structural comparison of the dorsal vessel in both life stages and highlight differences that may account for the markedly different hemolymph flow patterns observed between larval and adult mosquitoes.

RESULTS

The larval and adult heart lie along the dorsal midline, but the larval heart beats exclusively in the anterograde direction

To restrain larvae for video recordings, individuals were placed on a microscope slide in a pool of water between two coverslip stacks (Fig. 1A). Observation of the dorsal abdomen in fourth instar larvae revealed the presence of a dorsal vessel that runs the length of the body and is flanked by dorsal longitudinal tracheal trunks (Fig. 1B). Because of (1) the high visibility of the tracheal trunks under trans-brightfield illumination, (2) their location immediately lateral to either side of the dorsal vessel (which is fairly translucent under brightfield conditions) and (3) their rhythmic movement driven by each dorsal vessel contraction, the dorsal longitudinal tracheal trunks were used as a proxy for monitoring heart contractions. Brightfield intravital video recordings revealed that the larval heart beats at a more or less constant pace and only in the anterograde direction: each contraction originates at the posterior of the abdomen and propagates towards the head in a wave-like fashion (Fig. 1C; supplementary material Movie 1). Wave-like contractions of the larval heart alternate between periods of systole and diastole to propel hemolymph through the dorsal vessel in a bolus-like fashion. In all the videos recorded during the course of this study, the larval heart was never observed contracting in the retrograde direction.

Visualization of heart contractions in adult mosquitoes was carried out by brightfield trans-illumination of the abdomen using a non-invasive restraint technique described previously (Fig. 1D) (Andereck et al., 2010; Glenn et al., 2010). This method relies on the direct imaging of the heart through the relatively translucent abdominal tergum. Intravital recordings revealed that, as is the case with larvae, the adult heart extends along the dorsal midline of the entire abdomen (Fig. 1E). In contrast to the larval heart, the adult heart undergoes regular heartbeat directional reversals, beating for longer periods of time in the anterograde direction but switching to the retrograde direction at regular intervals (Fig. 1F). When compared with larvae, the adult heart appears to constrict more narrowly during systole, particularly when contracting in the retrograde direction.

The larval heart contracts at a slower rate than the adult heart, but neither is significantly affected by injury or injection

Initial visual observations of larval heart contractions suggested that the resting heart rate of larvae was significantly slower than that of adults. To confirm this, we performed intravital video imaging and measured the larval and adult heart rate in naïve mosquitoes, injured mosquitoes and mosquitoes that had been injected with either phosphate-buffered saline (PBS) or 2 µm diameter microspheres in PBS. Quantification of heart contractions in naïve fourth instar

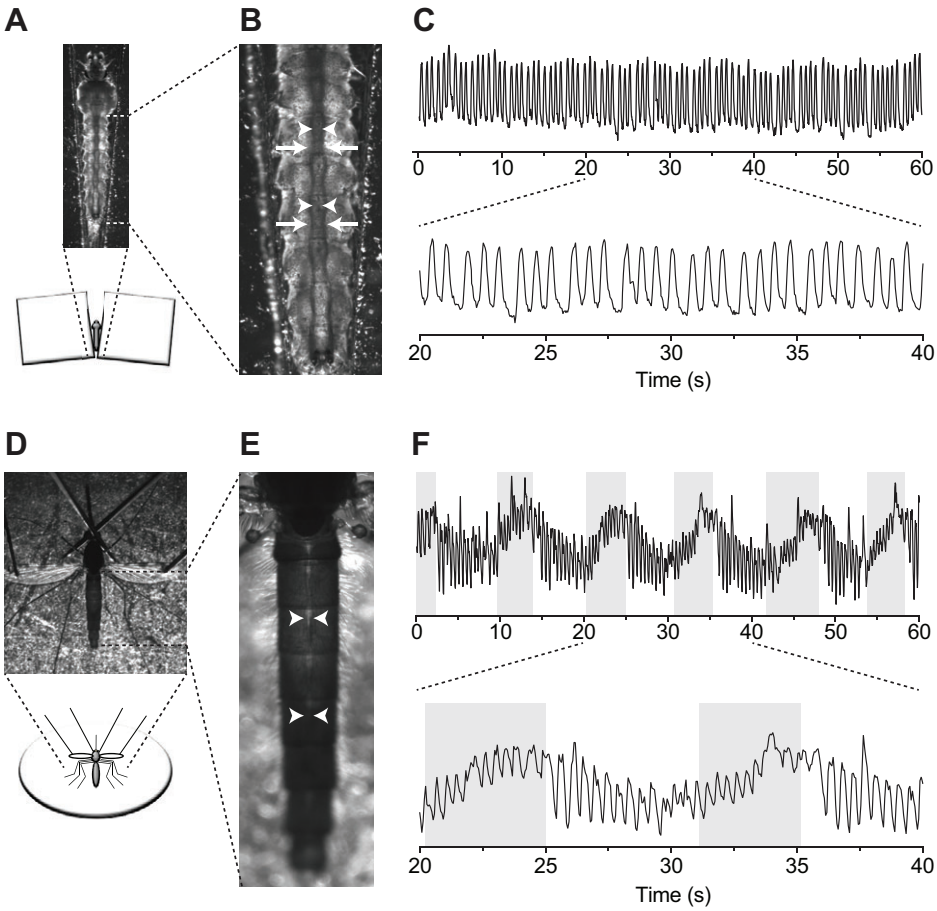

Fig. 1. Larval and adult heart contractions in *Anopheles gambiae*. (A) Larval restraint technique for brightfield intravital video recording of heart contractions. Larvae were restrained in water that was pooled between two stacks of coverslips. (B) Brightfield image of the larval abdomen showing that the heart (arrowheads) is located between the dorsal longitudinal tracheal trunks (arrows). (C) Graphical representation of larval heart contractions, where each peak represents a contraction. Contractions from the middle third of the 60 s recording are magnified in the lower graph. All larval contractions propagate in the anterograde direction. (D) Adult restraint technique for brightfield intravital video recording of heart contractions. Adults were cold-anesthetized and pins were placed through non-vascular portions of the wings and over the neck. (E) Brightfield image of the adult abdomen showing the heart (arrowheads). (F) Graphical representation of adult heart contractions, where each peak represents a heart contraction. Contractions from the middle third of the 60 s recording are magnified in the lower graph. Unshaded and shaded areas represent periods of anterograde and retrograde heart contraction, respectively.

The Journal of Experimental Biology (2015) doi:10.1242/jeb.114942

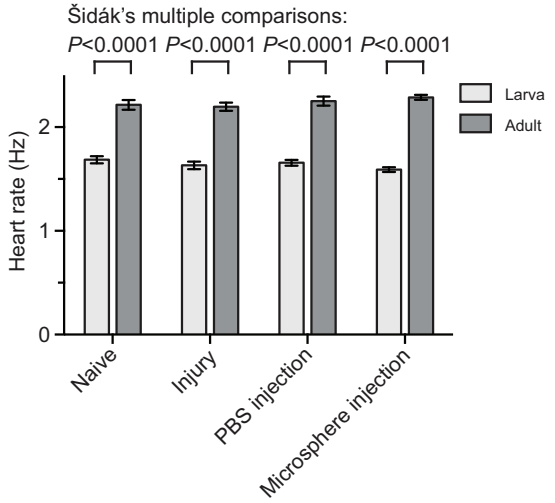

Fig. 2. Larval and adult heart contraction rates. Heart contraction rates were quantified in larvae and adults after receiving no treatment (naïve), a needle wound (injury), an injection with PBS, or an injection with 2 µm fluorescent microspheres in PBS. Across all comparisons, larvae displayed lower heart rates than adults (two-way ANOVA, $P<0.0001$), but treatment did not affect heart rates ($P=0.6725$). Whiskers denote the s.e.m.

larvae revealed that their heart contracts at an average resting rate of 1.69 Hz compared with 2.21 Hz in adults (Fig. 2). Statistical analysis of the data from all treatment groups confirmed that heart rates differ significantly between the two life stages (Fig. 2; two-way ANOVA, $P<0.0001$). Specifically, the heart rates from each of the four larval groups were significantly lower than the heart rates from the corresponding adult groups (Šidák multiple comparisons test, $P<0.0001$ for all comparisons). Moreover, treatment did not affect larval or adult heart rates (two-way ANOVA, $P=0.6725$), indicating that injury or injection has little or no effect on cardiac physiology. There was also no interaction between the life stage and the treatment, indicating that the life stages were not differentially affected by the injury or injection (two-way ANOVA, $P=0.1029$).

Hemolymph flow velocity through the dorsal vessel is significantly slower in larvae compared with adults

Because the larval heart contracts at a slower rate than the adult heart, we hypothesized that larval hemolymph flow velocity inside the dorsal vessel would also be slower. To test this hypothesis, larvae and adults were injected with identical solutions of 2 µm diameter red fluorescent latex microspheres, and the velocity of these microspheres was measured by intravital video imaging under low-level fluorescence illumination (Fig. 3A). Tracking of injected microspheres showed that intracardiac larval hemolymph travels at an average velocity of 2344 µm s^{-1}, whereas intracardiac hemolymph in adults travels in the anterograde and retrograde directions at velocities of 7420 and 7346 µm s^{-1}, respectively (Fig. 3C; supplementary material Movie 2; Dunn's test, $P<0.0001$ for both comparisons). This indicates that intracardiac hemolymph velocity is ~215% faster in adults when compared with larvae. Consistent with our previous findings (Glenn et al., 2010), hemolymph flow velocity in adults did not differ between periods of anterograde and retrograde flow (Dunn's test, $P>0.9999$). Furthermore, larval hemolymph travelled though the ventral hemocoel in the retrograde direction at an average velocity of 210 µm s^{-1}, which was an order of magnitude slower than intracardiac hemolymph flow and indicated that hemolymph

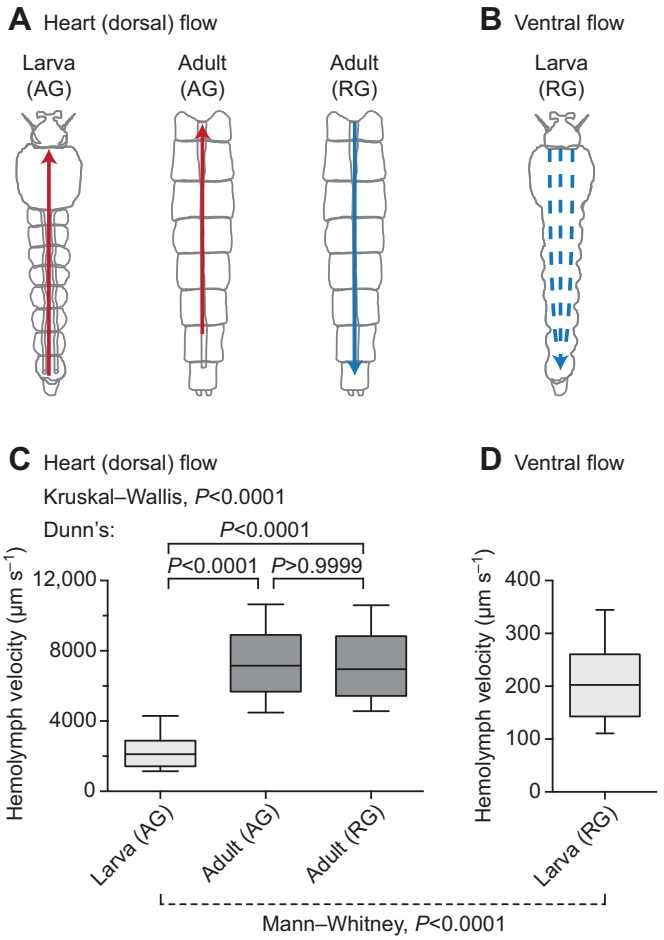

Fig. 3. Larval and adult hemolymph flow velocity. (A) Diagrammatic representation (dorsal view; anterior on top) of intracardiac hemolymph flow in larvae (left) and the adult abdomen (middle and right). Hemolymph inside the larval heart is only propelled in the anterograde direction (AG; red arrow) whereas hemolymph is propelled across the adult heart in both anterograde (red arrow) and retrograde (RG; blue arrow) directions. (B) Diagrammatic representation (ventral view) of extracardiac hemolymph flow in the larval ventral abdomen, showing that hemolymph only moves in the retrograde direction (blue arrows). (C) Hemolymph velocity in the heart of larvae and adults, as determined by the tracking of neutral density fluorescent microspheres. Intracardiac (anterograde) hemolymph in larvae travels significantly more slowly than intracardiac (anterograde and retrograde) hemolymph in adults. (D) Extracardiac retrograde hemolymph flow in the ventral abdomen of larvae. In larvae, extracardiac flow is significantly slower than intracardiac flow. For box plots, the center line marks the median, the box marks 50% of the data, and the whiskers mark 90% of the data.

dramatically slows upon exiting the dorsal vessel (Mann–Whitney test, $P<0.0001$; Fig. 3B–D; supplementary material Movie 3).

The larval heart is structurally similar to the adult heart, but its associated abdominal wall musculature and alary muscles differ drastically

The differences observed in larval and adult heart physiology probably result from underlying structural changes that occur during metamorphosis. To uncover these changes, we performed a structural analysis of the musculature associated with the dorsal abdomen of both larvae and adults. Specifically, we treated the dorsal abdomens with Alexa Fluor-conjugated phalloidin, which binds F-actin, and visualized the specimens by fluorescence microscopy.

The Journal of Experimental Biology (2015) doi:10.1242/jeb.114942

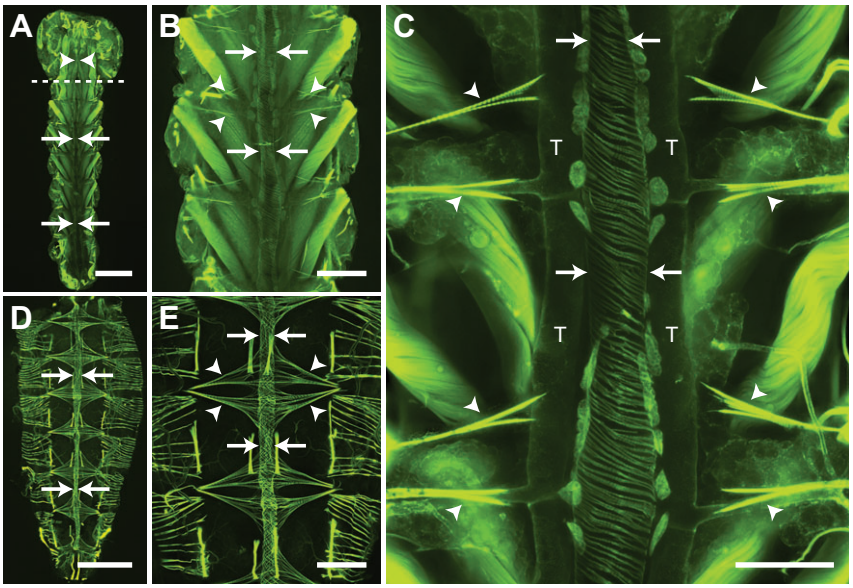

Fig. 4. Larval and adult heart structure. All images are fluorescence micrographs of specimens treated with Alexa Fluor conjugated phalloidin, which labels muscles green. (A) Image of the larval dorsal thorax and abdomen showing that the dorsal vessel extends the length of the body along the dorsal midline and is subdivided into an abdominal heart (arrows) and a thoracic aorta (arrowheads). The dashed line delineates the thoraco-abdominal junction. (B) A portion of the larval abdomen illustrated in panel A, magnified to show the heart (arrows) and associated alary muscles (e.g. arrowheads). The larval heart is flanked on either side by large swim muscles that approach the heart at ~45 deg angles. (C) High magnification view of two segments of the larval heart (arrows) showing the spiral arrangement of cardiomyocytes, the dorsal longitudinal tracheal trunks (T) and the alary muscles (arrowheads). Also visible along the surface of the heart are numerous pericardial cells. (D) Adult dorsal abdomen showing the heart (arrows), which runs the length of the abdomen along the dorsal midline. (E) A portion of the adult abdomen magnified to show the heart (arrows) and the extensive alary muscles (arrowheads). All images are oriented with anterior on top. Scale bars: A and D, 500 µm; B and E, 200 µm; C, 100 µm.

Muscle staining of the larval abdomen revealed a dorsal vessel consisting of an abdominal heart and a thoracic aorta that spans the length of the body along the dorsal midline (Fig. 4A). The larval heart is nestled within a thin dorsal cavity that is reminiscent of the adult pericardial sinus and is created by massive, segmentally arranged swim muscles that flank the heart and intersect it at nearly 45 deg angles (Fig. 4A–C). Under low magnification, the larval heart was often difficult to distinguish from the surrounding tissues because the fluorescence emitted by the heart, though similar to that of adults, was nearly overwhelmed by that of the surrounding swim muscles (Fig. 4A,B). The larval heart muscle is composed of a single layer of spirally arranged cardiomyocytes which, when viewed from the ventral side, form a clockwise, left-handed helical twist with respect to the lumen of the vessel (Fig. 4C). Three-dimensional rendering of deconvolved *Z*-stacks showed that the larval heart is dorsal and medial to the longitudinal tracheal trunks (supplementary material Movie 4).

Extending towards the dorsal midline from areas near the tergum–pleuron junction at a location that is immediately posterior to each abdominal suture are six complete and three incomplete pairs of bilaterally symmetrical alary muscles (Fig. 4B,C). These muscles attach to the heart on either side of the abdominal suture and tether it to the dorsal abdominal cuticle. The complete alary muscle pairs are located in abdominal segments 2–7. One incomplete alary muscle pair is located at the thoraco-abdominal junction and the other two are present at the posterior suture where the seventh and eighth abdominal segments are joined. Each alary muscle branches once, and each branch splits again to form two connections at the ventrolateral surface of the heart at a location near the pericardial cells. The points where the alary muscles connect to the heart were usually too tenuous to remain intact in our mounted specimens, but using a different imaging technique other researchers have observed the connection between the alary muscles and the heart of *A. aegypti* larvae (Leódido et al., 2013).

Consistent with our video recordings, muscle staining revealed that the larval and adult heart lie in the same location and span the same length along the dorsal midline of the abdomen (Fig. 4). However, comparative analyses revealed a significant disparity in overall abdominal musculature between the larva and adult stages. Specifically, compared with the larval swim muscles, the adult abdomen displays a significantly smaller array of intrasegmental lateral muscle fibers, which are oriented at 90 deg angles with respect to the heart (Fig. 4D,E). In both larvae and adults the structure of the heart varied depending on the contraction state at the time of fixation. However, the spiral arrangement of cardiomyocytes was similar in both life stages (Fig. 4).

Although the alary muscles of larvae and adults share the same point of origin at the body wall, alary muscle connections to the heart are far more extensive in adults when compared with larvae. In adults, each alary muscle branches once and then divides again to form anywhere from 10 to >30 myofiber connections to the heart. So extensive are these connections in adults that the anterior-most connection of one alary muscle extends to the posterior-most connection of the alary muscle located in the adjacent abdominal segment (Fig. 4D,E). Together, these structures form the basket-like muscular network that comprises the incomplete dorsal diaphragm in adults, a structure that is essentially absent in larvae due to their immature alary muscles.

Larval and adult abdominal ostia are in the same location and display a similar structure

The larval heart contains paired ostia, or valves, at the anterior portion of abdominal segments 2–7. An additional pair of ostia is located at the thoraco-abdominal junction, where the heart joins the aorta (discussed below). The ostia are located on the lateral sides of the heart near the anterior of each abdominal segment (Fig. 5A–C). Near each ostium is the junction of the posterior branch of each alary muscle, and each ostium is flanked ventrally by a pair of large pericardial cells (Fig. 4C; Fig. 5A). The heart muscle near the ostia typically bulges out slightly, giving the periostial regions a slightly wider diameter than other regions of the heart, perhaps due to increased tension created by the attachment of the alary muscles. Each ostium consists of two specialized cardiomyocytes that contain prominent nuclei and form funnel-shaped lips that extend into the lumen of the vessel (Fig. 5B,C).

The ostia of adults are also positioned at the anterior portions of abdominal segments 2–7 (Fig. 5D–F), suggesting that all of the larval abdominal ostia are maintained into adulthood. Likewise, adult abdominal ostia form funnel-shaped lips that protrude into the heart lumen in an anterior direction and contain paired nuclei (Fig. 5E,F). Although the muscle that comprises these lips was occasionally observed in larval ostia, it was significantly more

The Journal of Experimental Biology (2015) doi:10.1242/jeb.114942

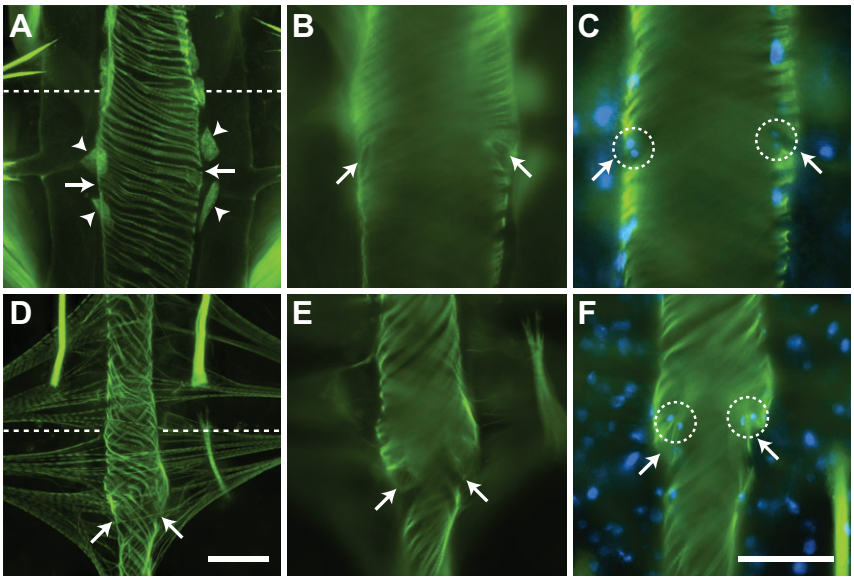

Fig. 5. Larval and adult abdominal ostia. Phalloidin stained larval (A–C) and adult (D–F) hearts showing the location and structure of the ostia. (A) Larval ostia (arrows) are located on the lateral sides of the heart in between and dorsal to a pair of enlarged pericardial cells (arrowheads). (B) Ostia (arrows) are oriented towards the anterior of the organism as they extend into the lumen of the vessel. (C) Each ostium (arrows) is composed of a pair of cardiomyocytes (nuclei are labelled blue with Hoechst 33342; circles). (D) Adult ostia (arrows) are located on the lateral sides of the heart near the posterior of each alary muscle pair. Pericardial cells are present but are not labelled. (E) Ostia (arrows) are oriented towards the anterior of the organism as they extend into the lumen of the vessel. (F) Each ostium is composed of two cardiomyocytes (nuclei are labelled blue; circles). Note how the ostia extend into the lumen of the vessel (arrows). All images are oriented with anterior at the top, and the abdominal sutures are marked with a dashed line. Scale bars: A and D, 50 µm; B, C, E and F, 50 µm.

prominent in adults. Furthermore, larval ostial nuclei were typically found closer to the heart wall rather than projecting into the lumen.

Larval hemolymph enters the dorsal vessel primarily through incurrent openings in the eighth abdominal segment and not the abdominal ostia

Intravital video imaging revealed that 2 µm diameter red fluorescent microspheres injected into the larval ventral hemocoel migrate slowly in the retrograde direction, bypass the abdominal ostia and enter the dorsal vessel at the posterior terminus of the heart (Fig. 3B; supplementary material Movie 5). To gauge the amount of hemolymph that enters the larval heart through the terminal opening in the eighth abdominal segment relative to the ostia located in abdominal segments 2–7, microspheres were injected into the larval thorax and the number of microspheres that entered the dorsal vessel within each abdominal segment over a 60 s time period was quantified. Although microspheres were occasionally observed entering the heart through the abdominal ostia, the vast majority of microspheres (>99%) entered the dorsal vessel through the terminal openings of the heart in the eighth abdominal segment (Wilcoxon matched pairs test, $P<0.0001$; Fig. 6). Even when injecting larvae with higher concentrations of fluorescent microspheres, regardless of the site of injection, the microspheres consistently migrated posteriorly and only entered the dorsal vessel after reaching the eighth abdominal segment.

The larval posterior incurrent openings of the heart are structurally similar to the adult excurrent openings

Examination of the anterior portion of the eighth abdominal segment of phalloidin-treated larvae revealed the structure of the posterior terminus of the heart (Fig. 7A–E). This structure consists of two incurrent openings that allow hemolymph to enter the lumen of the dorsal vessel (Fig. 7C). The cardiomyocytes that form these openings create a laterally oriented figure-of-eight and coalesce at the center of the heart lumen to form a thin but dense structure that protrudes from the heart and attaches to the body wall (Fig. 7A–E). The larval incurrent openings are further supported by two sets of incomplete alary muscles (Fig. 7A,B,D,E), as well as by extensive connections with tracheal tufts that originate near the dorsal longitudinal tracheal trunks at the posterior of the eighth abdominal segment (Fig. 7D–F). The tracheal tufts are a dense mass of thin trachea that is suspended in the hemolymph and shifts with each heart contraction.

The posterior terminus of the adult heart is exclusively excurrent (Glenn et al., 2010), and thus serves the opposite function to the one

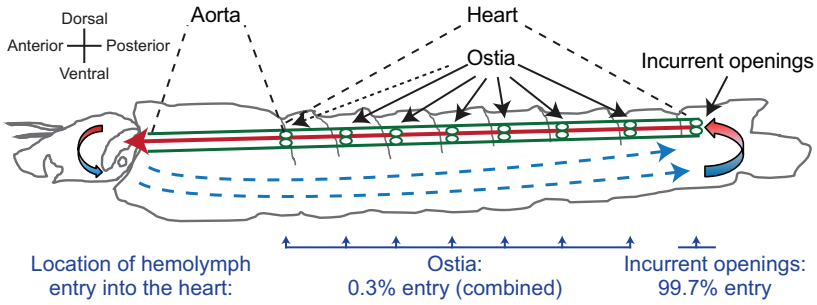

Fig. 6. Larval hemolymph flow patterns and entry through the eighth abdominal segment incurrent openings of the heart. Diagrammatic representation (lateral view) of hemolymph flow in larvae. Hemolymph enters the dorsal vessel (green) at the posterior terminus of the heart in the eighth abdominal segment and travels rapidly in the anterograde direction (red arrow) before exiting the aorta near the head. After exiting the aorta, hemolymph flows slowly in the extracardiac hemocoel in the retrograde direction (blue arrows) and then re-enters the dorsal vessel via a pair of incurrent openings at the posterior terminus of the heart. This diagrammatic representation was constructed after visualizing the movement of fluorescent microspheres that had been injected into the hemocoel. The bottom of the image displays the percentage of microspheres that enter the heart through the ostia and the percentage of microspheres that enter the heart through the incurrent openings located at the posterior terminus of the heart (Wilcoxon matched pairs test, $P<0.0001$). The ostia and incurrent openings are labelled with continuous arrows and the thoraco-abdominal ostia are labelled with a dashed arrow.

The Journal of Experimental Biology (2015) doi:10.1242/jeb.114942

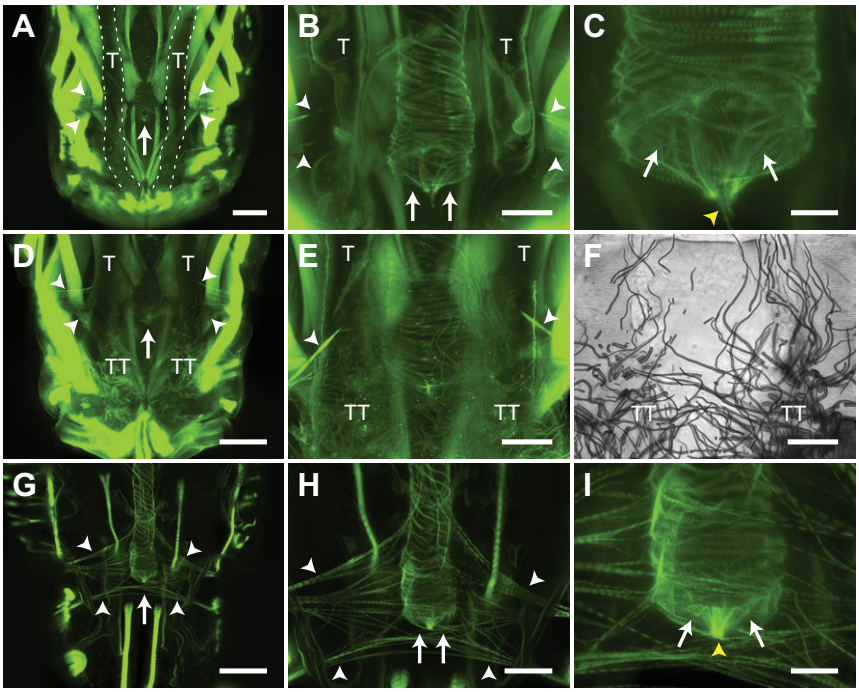

Fig. 7. Larval and adult posterior heart structure. (A–C) Image series showing, in increasing magnification, phalloidin staining of the larval posterior incurrent openings of the heart. The posterior terminus of the larval heart ends in the anterior portion of the eighth abdominal segment, lies between the dorsal longitudinal tracheal trunks (T), and is supported by two incomplete pairs of alary muscles (white arrowheads). The posterior terminus of the larval heart contains two incurrent openings (arrows) that contain a muscular tether (yellow arrowhead) that attaches the heart to the abdominal wall. (D–F) Series of fluorescence (D,E) and brightfield (F; same specimen as E) images showing that the posterior terminus of the larval heart is also attached to an extensive network of thin tracheoles called the tracheal tufts (TT), which extend from a location near the posterior base of the dorsal longitudinal tracheal trunks (T). (G–I) Image series showing, in increasing magnification, phalloidin staining of the adult posterior excurrent openings of the heart. The posterior terminus of the adult heart ends in the anterior portion of the eighth abdominal segment and is supported by two incomplete pairs of alary muscles (white arrowheads). The posterior terminus of the adult heart contains two excurrent openings (arrows) that contain a muscular tether (yellow arrowhead) that attaches the heart to the abdominal wall. All images are oriented with anterior at the top. Scale bars: A, D and G, 100 µm; B, E, F and H, 50 µm; C and I, 20 µm.

found in larvae. The adult posterior heart shares the same paired openings as the larval posterior heart, as well as a similar point of attachment to the body wall (Fig. 7G–I). Also similar to larvae, the adult posterior terminus of the heart is supported by two sets of incomplete alary muscles, although, as is the case with the other alary muscles, these form more extensive connections to the heart in adults when compared with larvae.

The larval aorta extends from the thoraco-abdominal junction to the base of the head and differs in structure from the heart

Imaging of the larval thoracic musculature after phalloidin staining revealed the presence of a thoracic aorta that extends from the thoraco-abdominal junction to the anterior portion of the thorax (Fig. 8A). The shape of the aorta varies substantially depending on

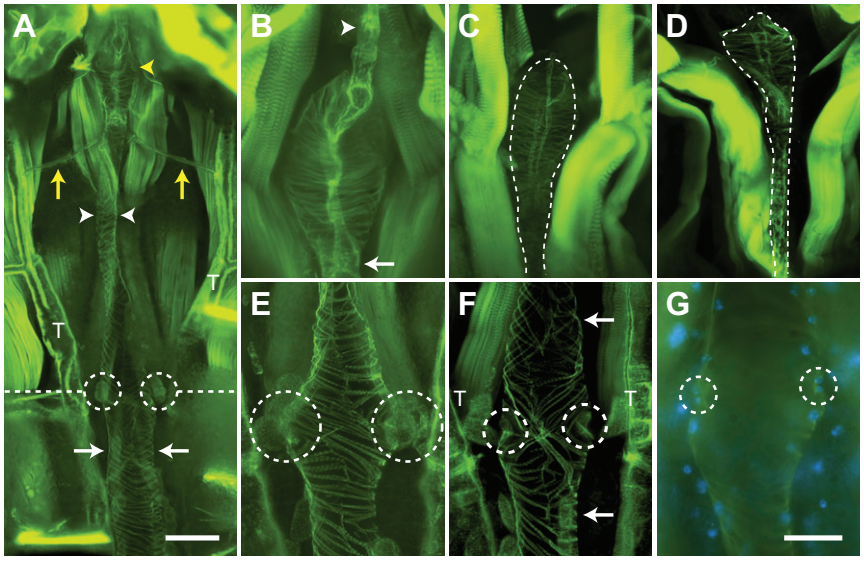

Fig. 8. Larval aorta structure. (A) Phalloidin staining of muscle showing the anterior portion of the abdominal heart (arrows), the thoraco-abdominal junction (dashed line), the ostial pair at this junction (circles), the dorsal longitudinal tracheal trunks (T), the thoracic aorta (arrowheads), prominent trachea that attach to the aorta (yellow arrows), and the bulbous chamber of the aorta (yellow arrowhead). (B–D) Series of images showing the anterior bulbous chamber of the aorta. (B) The aorta forms a dense neck region posterior to the bulbous chamber (arrow), which widens significantly into a bulbous chamber before narrowing once again into a thin muscular siphon (arrowhead), where hemolymph passes through prior to emptying into the head. (C,D) The aorta, depending on the contraction state of the heart, varies greatly in shape, widening in response to a heart contraction (C) and narrowing during relaxation (D). (E–G) Series of images showing the structure of the thoraco-abdominal junction. (E) The diamond-shaped thoraco-abdominal junction displays a knot-like arrangement of cardiomyocytes in both left- and right-handed helical orientations and contains two ostia (circles). (F) The regular left-handed helical arrangement of heart cardiomyocytes (bottom arrow) differs from the irregular arrangement of both left- and right-handed helices in aorta cardiomyocytes (top arrow). The ostia at the thoraco-abdominal junction can be seen as invaginations (circles) in the cardiac muscle. (G) Each ostium at the thoraco-abdominal junction contains paired cardiomyocyte nuclei (blue; circles) that lie at the periphery of the heart lumen. All images are oriented with anterior at the top. Scale bars: A, 100 µm; B–G, 50 µm.

the contraction state of the heart; during contraction, the aorta widens (Fig. 8B,C), while during relaxation the aorta narrows (Fig. 8D). Although no alary muscle attachments were observed supporting the aorta, two prominent trachea that originate from the longitudinal tracheal trunks were seen attached to the anterior portion of the vessel, perhaps providing structural support in addition to meeting oxygen demands (Fig. 8A).

At the thoraco-abdominal junction, the heart portion of the larval dorsal vessel forms a diamond-shaped structure reminiscent of the 'conical chamber' described in adult *Drosophila* (Fig. 8A,E–G) (Wasserthal, 2007). The cardiac musculature at the 'conical chamber' forms an irregular knot-like shape consisting of cardiomyocytes in both left- and right-handed helical orientations, which is different from the regular left-handed helical arrangement found throughout the heart (Fig. 8A,E,F). Also in contrast to the cardiomyocytes of the heart, the region of the aorta that is anterior to the thoraco-abdominal junction displays an irregular arrangement of cardiomyocytes that includes longitudinal seams along the dorsal and ventral midlines of the aorta (Fig. 8E,F). These seams form due to the junction of lateral aorta muscles of opposite helical orientation.

Although the aorta proper, unlike the heart, does not contain ostia, a pair of ostia is present at the thoraco-abdominal junction (Fig. 8E–G). As with the abdominal ostia, each thoraco-abdominal ostium is flanked ventrally by pericardial cells and is composed of two specialized cardiomyocytes whose nuclei are found near the perimeter of the vessel wall. Lip-forming muscle projections were difficult to visualize in larvae, although lip-like invaginations typical of abdominal ostia were routinely observed (Fig. 8F). Unlike adults, where the thoraco-abdominal ostia accept extracardiac hemolymph during periods of retrograde heart flow (Glenn et al., 2010), the thoraco-abdominal ostia of larvae were largely inert.

The aorta narrows significantly as it extends from the thoraco-abdominal junction to the anterior of the thorax. As it approaches the anterior portion of the thorax it widens once again to form a bulbous chamber that displays a circular arrangement of cardiomyocytes and can approximate the diameter of the heart. This bulbous chamber, previously described as the 'prothoracic aortic sinus' in *Anopheles quadrimaculatus* (Jones, 1954), begins with a dense neck region before widening and then tapering off ventrally into a narrow, muscular siphon, which hemolymph passes through just prior to exiting into the head (Fig. 8A,B). Intravital imaging near the base of the head confirmed the presence of the excurrent opening of the aorta, which releases hemolymph into the head where it remains briefly before gradually flowing in the posterior direction (supplementary material Movie 6). Although hemolymph flow patterns in adults suggest a similar location and function of the adult aorta and anterior excurrent opening, no reliable images of these structures have been obtained (Glenn et al., 2010).

DISCUSSION

The comparative structural and functional data presented herein advance our understanding of the insect circulatory system by providing novel insights into its development across the life stages of the African malaria mosquito, *A. gambiae*. Overall, the larval pattern of unidirectional heart contraction and hemolymph flow reflects a simpler version of the adult circulatory system, a difference in complexity that is probably a function of the more streamlined body plan and overall morphology of the larval life stages. Likewise, the increased complexity of the adult circulatory system may reflect adaptations to the morphology and physiological demands specific to the adult stage, such as those involved in flight, blood feeding and reproduction.

In this study we found that while the adult heart contracts in both the anterograde and retrograde directions, the larval heart only contracts in an anterograde direction. Unidirectional anterograde heart contraction is a common feature of insect larvae (Gerould, 1924; Jones, 1954; Jones, 1977; Miller, 1985; Smits et al., 2000; Dulcis et al., 2001; Sláma and Farkas, 2005). Heartbeat directional reversals, however, have been observed primarily in adult insects from a variety of holometabolous orders, with contraction reversals generally beginning either at the adult stage or around the time of pupation (Gerould, 1933; Miller, 1997). Although the late-stage larvae of some insects undergo heartbeat reversals prior to pupation (Gerould, 1933; Matsushita et al., 2002; Uchimura et al., 2006), we never observed mosquito larvae, even when nearing pupation, undergoing heartbeat directional reversals. The reason mosquito adults, but not larvae, undergo periodic heartbeat directional reversals remains unknown, but in other insects several environmental and neural stimuli are known to control contraction directionality. For example, the larval heart of *Manduca sexta* contracts only in the anterograde direction whereas the pupal and adult heart periodically reverses contraction direction (Davis et al., 2001). The rhythmicity of adult heartbeat reversals is altered by tactile stimuli, eliminated by the treatment with tetrodotoxin (a neurotoxin), and controlled by specific motor neurons (Dulcis et al., 2001). Neural and hormonal stimuli also modulate the proportional directionality of heart contractions in other insects (Kuwasawa et al., 1999; Dulcis et al., 2005; Dulcis and Levine, 2005), indicating that although the insect heart is myogenic (Jones, 1977; Chapman et al., 2013; Klowden, 2013), contraction dynamics are under partial neural control. In *D. melanogaster*, anterograde heart contractions are thought to be modulated by a putative pacemaker located at the posterior end of the heart (Dulcis and Levine, 2003), whereas retrograde heart contractions are thought to be modulated by a pacemaker located in the conical chamber, which represents the anterior-most region of the heart (Dulcis and Levine, 2005). This conical chamber develops during metamorphosis, and thus is not present in larvae (Curtis et al., 1999; Dulcis and Levine, 2003), suggesting that the larval heart may lack the inherent ability to contract in the retrograde direction. Indeed, the larval heart of most insects appears to lack direct innervation and the formation of an anterior retrograde pacemaker in adults probably coincides with the formation of new neuronal inputs during metamorphosis to co-ordinate the action of the anterograde and retrograde pacemakers (Davis et al., 2001; Dulcis et al., 2001; Dulcis and Levine, 2003; Dulcis and Levine, 2004; Dulcis and Levine, 2005). This notion is consistent with the findings of the present study as well as our recent studies that have shown that the adult heart of *A. gambiae* is both innervated and under partial hormonal control, with the identified cardiomyotropic neuropeptides having a stronger effect during periods of anterograde heart contraction (Chen and Hillyer, 2013; Estévez-Lao et al., 2013; Hillyer et al., 2014).

The finding that the larval mosquito heart contracts more slowly than the adult heart is consistent with earlier findings in *A. quadrimaculatus* (Jones, 1954) as well as the increased 'fast forward' phase beating that occurs in *M. sexta* following eclosion (Smits et al., 2000; Dulcis et al., 2001). Similarly, the heart rate of *Drosophila* adults is approximately double that of the third instar larvae (Sláma and Farkas, 2005). We also observed that hemolymph flow velocity was slower in larvae compared with adults, with intracardiac larval hemolymph travelling at less than one-third of the speed of intracardiac hemolymph flow in adults. Because this slower flow velocity correlates with a slower contraction rate in larva when compared with adults, it appears that the more rapid heart rate in

adults allows this life stage to propel hemolymph at vastly greater velocities than larvae. Furthermore, as systole appears to constrict the heart of adults to a greater degree than occurs in larvae, the increased reduction in heart luminal volume that presumably accompanies each adult contraction may explain why the developmentally associated increase in intracardiac hemolymph velocity is much greater than the increase in the heart rate (~215% versus ~30%, respectively).

The relative paucity of abdominal body wall musculature in adults compared with larvae indicates a drastic reduction in muscle mass after metamorphosis. However, despite lying in the center of and in close proximity to these abdominal wall muscles, both the larval and adult hearts: (1) are composed of a thoracic aorta and an abdominal heart; (2) span the same length along the dorsal midline of the abdomen; (3) display the same spiral arrangement of cardiomyocytes; (4) contain the same number of ostia; and (5) retain ostia in the same position and at regular intervals that closely align with the anterior portion of each abdominal segment. Together with the fact that larvae and adults have the same number of abdominal segments, these findings suggest that all portions of the larval heart are maintained following eclosion. In contrast to this high degree of continuity, the adult dorsal vessel in *Drosophila* differs greatly from its larval predecessor in each of the aforementioned areas: (1) unlike adults, the larval aorta spans both thoracic and abdominal segments (T3 to A5) (Curtis et al., 1999; Molina and Cripps, 2001; Wasserthal, 2007); (2) the posterior two segments of the larval heart are lost during metamorphosis (Curtis et al., 1999; Molina and Cripps, 2001; Lehmacher et al., 2012); (3) unlike the regular circular arrangement of adult cardiomyocytes, the larval heart contains a mixture of both circular and helically oriented muscles (Lehmacher et al., 2012); (4) only the first of the three larval ostial pairs are retained into adulthood, with four additional pairs arising during metamorphosis from progenitor cells in the larval aorta (Curtis et al., 1999; Molina and Cripps, 2001; Wasserthal, 2007); and (5) the ostia and the alary muscles of both larvae and adults are not evenly spaced across the abdominal segments. This extensive restructuring of the *Drosophila* dorsal vessel, which is absent in mosquitoes, may be due to the greater disparity between the larval and adult body plans of *Drosophila* when compared with *A. gambiae*, whose larvae and adults, unlike *Drosophila*, both have a distinct head, thorax and abdomen.

In contrast to the relative stability of the heart across mosquito life stages, the supporting alary muscles are grossly under-developed in larvae when compared with adults, an observation recently made across life stages in *A. aegypti* (Leódido et al., 2013) that is also consistent with structural data from adults of other mosquito species (Martins et al., 2011). This disparity in alary muscle support may partly account for the differences in contraction and hemolymph flow dynamics observed between the two life stages, as alary muscles are believed to not only aid in the relaxation of the heart muscle during diastole (Lehmacher et al., 2012) but also to facilitate the opening and closing of the ostia (Glenn et al., 2010). During our particle-tracking experiments we observed that nearly all of the injected microspheres entered the lumen of the larval dorsal vessel through the posterior incurrent openings of the heart instead of the ostia, a finding that is in agreement with indirect observations in *A. quadrimaculatus* larvae (Jones, 1954). Although larval ostia typically contained lips that were less prominent than those of adults and lay close to the perimeter of the heart, thus resembling ostia in the 'closed' position, the orientation of larval ostia towards the anterior of the insect is consistent with their eventual function in the adult stage as incurrent valves for hemolymph entry into the heart during periods of anterograde heart contractions (Jones, 1977; Glenn et al., 2010). Furthermore, as microspheres occasionally (though rarely) entered the larval heart through the abdominal ostia, we hypothesize that the developmental differences in the mechanics of hemolymph entry into the dorsal vessel are not due to major stage-specific structural differences in the ostia themselves but instead due to differences in the degree of nearby alary muscle support. Indeed, the ostia described here appear to be both developmentally and evolutionarily conserved, as structurally similar ostia have been described in both the larval and adult stages of *A. aegypti* (Leódido et al., 2013) and *Drosophila* (Curtis et al., 1999; Molina and Cripps, 2001; Wasserthal, 2007; Lehmacher et al., 2012).

We have also shown that the function of the posterior terminus of the heart changes with developmental stage: larvae have incurrent openings whereas adults have excurrent openings. Incurrent function of the posterior larval heart has been inferred from observations in *A. quadrimaculatus* (Jones, 1954), and described in *Drosophila* (Babcock et al., 2008), as well as in some lepidopteran larvae (Locke, 1997; Rao et al., 2009). Each of these insect orders contains several known examples of adults with excurrent posterior heart function, suggesting that the functional change of the posterior terminus of the heart is evolutionarily conserved (Wasserthal, 1980; Wasserthal, 1981; Wasserthal, 2007; Glenn et al., 2010; Wasserthal, 2012). In *A. gambiae*, the posterior end of the heart is structurally similar in both larvae and adults, and the excurrent function that develops following eclosion is a direct result of the onset of retrograde heart contraction periods. The reason the posterior opening of the adult heart does not retain incurrent function even during periods of anterograde heart contractions remains unknown, but it is possible that the high efficiency of the adult abdominal ostia, which are inert in the larvae, has rendered posterior incurrent function unnecessary.

This study also provides the first structural description of the aorta of *A. gambiae*, as this portion of the dorsal vessel has proved difficult to visualize in adults due to its location in the highly sclerotized thorax (Glenn et al., 2010). The aorta differs significantly from the heart in the arrangement of its cardiomyocytes; whereas the heart contains regular, spirally arranged cardiomyocytes that form a left-handed helical twist, the aorta displays muscle cells arranged in both right- and left-handed helices. This distinct arrangement of cardiomyocytes may contribute to the capacity of the aorta for dramatic alterations in its diameter in response to heart contractions. Although similar irregularities in cardiomyocyte orientation have been noted in the heart and aorta of *Drosophila* larvae (Lehmacher et al., 2012), in mosquito larvae we found these irregularities exclusively in the aorta. However, the narrow diameter of the mosquito aorta and its lack of ostia are common features among insect aortas, including that of *Drosophila* (Jones, 1954; Molina and Cripps, 2001; Wasserthal, 2007; Lehmacher et al., 2012; Chapman et al., 2013).

Hemolymph circulation is an essential yet understudied aspect of insect biology and has been shown to influence thermoregulation, tracheal ventilation and the transport of nutrients, waste, hormones and immune factors (Wasserthal, 1999; Wasserthal, 2003; Babcock et al., 2008; Nation, 2008; Harrison et al., 2012; King and Hillyer, 2012; Wasserthal, 2012; Klowden, 2013). The present study on the circulatory system of *A. gambiae*, a primary disease vector of malaria in sub-Saharan Africa, increases our understanding of key physiological processes in this epidemiologically important mosquito. Specifically, the data presented herein provide novel insights into larval circulatory physiology and describe numerous differences between the larval and adult dorsal vessel, providing a

The Journal of Experimental Biology (2015) doi:10.1242/jeb.114942

developmental perspective on this organ system. Larvae are a common target in mosquito control strategies (Fillinger and Lindsay, 2011) and many chemical and biological pesticides exert their effect at the larval stage after penetrating the cuticle or midgut and circulating throughout the hemocoel (Favia et al., 2007; Otieno-Ayayo et al., 2008; Paily et al., 2012). Furthermore, numerous mosquito-borne pathogens must complete an obligate migration from the midgut to the salivary glands that involves traversing the hemocoel, where they are subject to hemolymph flow currents (Hillyer et al., 2007). Thus understanding both larval and adult circulatory physiology can yield important insights into current control methods as well as inform the creation of novel ones.

MATERIALS AND METHODS

Mosquito rearing and maintenance

Anopheles gambiae Giles *sensu stricto* (G3 strain; Diptera: Culicidae) were reared as described (Estévez-Lao et al., 2013). Briefly, eggs were hatched in distilled water and larvae were fed a combination of Koi food and yeast. Upon pupation, mosquitoes were transferred to plastic containers with a marquisette top where adults emerged and were fed a 10% sucrose solution *ad libitum*. All mosquito stages were maintained in an environmental chamber set to 27°C and 75% relative humidity under a 12 h:12 h light:dark photoperiod. All experiments were performed on fourth instar larvae and adult female mosquitoes at 5 days post-eclosion.

Mosquito injection

Larvae were immobilized by removing excess water and were then injected at the mesothorax with either ~0.1 µl PBS (pH 7.0) or 0.008% solids 2 µm diameter red fluorescent (580/605) carboxylate-modified microspheres (Invitrogen, Carlsbad, CA, USA) in PBS. Injured and naïve larvae received a needle wound or no treatment at all, respectively. Larvae were restrained for video recording by placing them in water that was pooled between two stacks of coverslips that were resting on a glass slide (Fig. 1A). This mode of restraint maintains anopheline larvae in their natural horizontal orientation with respect to the water surface. In these experiments, larvae had access to oxygen but in some cases they remained completely submerged during video recording. Thus it is possible that in these cases the restraint method limited the access of larvae to oxygen. However, it is highly unlikely that the restraint method had any effect on the larval heart for two reasons. Firstly, larvae were restrained for only a brief period (~90 s) and their heart rates did not change during the 60 s heart recording. Secondly, anopheline larvae often subject themselves to extensive anoxic conditions due to foraging as well as their 'flight' response, where they swim to the bottom of the larval pool and remain immobile until the perceived threat has disappeared.

Adult mosquitoes were cold-anesthetized prior to injection and restrained dorsal-side up on Sylgard 184 silicone elastomer (Dow Corning Corporation, Midland, MI, USA) plates using a non-invasive method previously described (Fig. 1D) (Andereck et al., 2010; Glenn et al., 2010). After acclimating to room temperature, adults were subjected to the same treatments as the larvae, with injections taking place at the thoracic anepisternal cleft.

Measurement of heart contractions

Immediately after treatment (naïve, injury or injection), 60 s intravital videos of the dorsal abdomen of larvae and adult mosquitoes were recorded under brightfield trans-illumination using a Nikon SMZ1500 stereo microscope (Nikon, Tokyo, Japan) connected to a Hamamatsu ORCA-Flash 2.8 digital CMOS camera (Hamamatsu Photonics, Hamamatsu, Japan) and Nikon Advanced Research NIS-Elements software. Videos were captured at ~20 frames s^{-1} and manually analysed using NIS-Elements software. Larval heart rates were quantified by visualizing the movement of the dorsal tracheal trunks, a technique previously employed to measure heart rates in *Drosophila* larvae (Dasari and Cooper, 2006). Adult heart rates were quantified by visualizing the direction and frequency of wave-like contractions of cardiac muscle throughout the length of the abdomen (Glenn et al., 2010). Because the heart rate in adult mosquitoes does not differ between anterograde and retrograde contraction periods (Glenn et al., 2010; Hillyer et al., 2012; Chen and Hillyer, 2013; Estévez-Lao et al., 2013), only adult total contraction rates are presented. Four independent trials of 10 individuals per treatment group were conducted. Data were analysed by two-way ANOVA, using stage and treatment as the variables, followed by Šidák's *post-hoc* test.

Graphical representations of individual larval heart contractions were rendered using NIS-Elements software by selecting an area of the heart immediately medial to the longitudinal tracheal trunks and quantifying how the sum light intensity changed as each heart contraction shifted the trachea in and out of the selected area. Graphical representations of individual adult heart contractions were rendered by selecting an area immediately medial to the dorsal diaphragm at the anterior-most region of the abdomen and quantifying changes in sum light intensity as the heart wall moved in and out of the selected area. For visualization ease, all values were multiplied by −1 such that each peak (not valley) signified a contraction.

Measurement of hemolymph flow velocity

Adults and larvae were restrained and injected as described above. For dorsal, intracardiac particle tracking, mosquitoes were injected with ~0.1 µl of 0.008% solids 2 µm diameter red fluorescent microspheres in PBS whereas for ventral, extracardiac particle tracking they were injected with 0.004% solids microspheres. Immediately following injection, adults and larvae were video recorded for 60 s using low-level fluorescence illumination on the SMZ1500 microscope ensemble described above.

Larval videos were acquired through the dorsal and ventral abdomen using either the Hamamatsu ORCA-Flash 2.8 digital CMOS camera or a Photometrics CoolSNAP HQ2 high sensitivity monochrome CCD camera (Roper Scientific, Ottobrunn, Germany) at 20–25 frames s^{-1}. The manual feature of the Object Tracker module of NIS-Elements was used to quantitatively track the trajectory of the neutral density microspheres as they flowed through the dorsal vessel or the ventral hemocoel. Hemolymph flow velocity was calculated from these measurements by dividing the path length of an individually tracked microsphere by the amount of time it was tracked. For each larva assayed, five microspheres were tracked as they travelled through the heart or through the ventral abdomen. A total of 40 larvae were assayed: 20 were assayed dorsally and 20 were assayed ventrally.

Videos of adult mosquitoes were acquired using the Photometrics CoolSNAP HQ2 camera at 24 frames s^{-1}. A total of 20 adult mosquitoes were assayed, and for each individual 10 microspheres were tracked: five as they travelled in the anterograde direction and five as they travelled in the retrograde direction. All microspheres were tracked for a minimum distance of 500 µm. Particle tracking data were analysed using the Kruskal–Wallis test, followed Dunn's multiple comparisons *post-hoc* test.

Quantification of hemolymph flow into the larval ostia and eighth abdominal segment incurrent openings

Larvae were injected with 0.008% solids 2 µm diameter red fluorescent microspheres in PBS and video recorded for 60 s using low-level fluorescence illumination on the SMZ1500 microscope equipped with the Photometrics CoolSNAP HQ2 camera. The number of fluorescent microspheres entering the dorsal vessel through the incurrent openings of the eighth abdominal segment and the abdominal ostia of segments 2–7 were manually counted. Twenty mosquitoes were assayed and the raw data were analysed using the Wilcoxon matched pairs test.

Light and fluorescence microscopy of aldehyde-fixed mosquito whole mounts

For fluorescence labelling of larval muscle, whole larvae were first fixed by immersion in 8% formaldehyde (Electron Microscopy Sciences, Hatfield, PA, USA) in PBS for 1 h. The larval thorax and abdomen were then bisected along a coronal plane, cleared of all internal organs, rinsed in PBS, and incubated for 1 h in a solution consisting of 0.3 µmol l^{-1} phalloidin-Alexa Fluor 488 (Invitrogen) and 1% Triton X-100 (Thermo Fisher Scientific, Waltham, MA, USA) in PBS. After rinsing in PBS, specimens were mounted on glass slides using Aqua-Poly/Mount (Polysciences Inc., Warrington, PA, USA).

For fluorescence labelling of adult muscle, adults were intrathoracically injected with 4% formaldehyde in PBS and allowed to fix for 15 min. Abdomens were bisected along a coronal plane and, after removal of internal organs, placed in 0.5% Tween in PBS for 15 min, rinsed three times briefly in PBS, fixed in 4% formaldehyde for 5 min, and incubated for 1 h in 0.3 µmol l^{-1} phalloidin-Alexa Fluor 488 and 1% Triton in PBS. After rinsing in PBS, adult dorsal abdomens were mounted on a glass slide using Aqua-Poly/Mount. For some adult and larval preparations, cell nuclei were fluorescently labelled by adding Hoechst 33342 (Invitrogen) to the phalloidin-containing solution.

Larval and adult samples were imaged under brightfield and fluorescence illumination using a Nikon 90i compound microscope connected to a Nikon Digital Sight DS-Qi1Mc monochrome digital camera. For the rendering of detailed fluorescence images with extended focal depth, *Z*-stacks of whole mounts were acquired using a linear encoded *Z*-motor and all images in a stack were combined to form a single focused image using the Extended Depth of Focus (EDF) module of NIS-Elements. For three-dimensional rendering, *Z*-stacks were created by acquiring images at 0.5 µm *Z*-intervals for a total *Z*-range of 30 µm. *Z*-stacks were then quantitatively deconvolved using the AQ 3D Blind Deconvolution module of NIS-Elements and rendered using the volume view feature.

Acknowledgements
We thank Tania Estevez-Lao for rearing the mosquitoes used in this study.

Competing interests
The authors declare no competing or financial interests.

Author contributions
G.P.L. and J.F.H. designed the experiments. G.P.L. and O.C.O. performed the experiments. G.P.L. and J.F.H. analysed the data and wrote the manuscript.

Funding
This research was funded by US National Science Foundation (NSF) grant IOS-1257936 to J.F.H. The NSF had no role in study design, data collection and analysis, decision to publish, or preparation of this manuscript. O.C.O. participated through the School for Science and Math at Vanderbilt, which is supported by award R25RR024261 from the National Center for Research Resources.

Supplementary material
Supplementary material available online at
http://jeb.biologists.org/lookup/suppl/doi:10.1242/jeb.114942/-/DC1

References

Andereck, J. W., King, J. G. and Hillyer, J. F. (2010). Contraction of the ventral abdomen potentiates extracardiac retrograde hemolymph propulsion in the mosquito hemocoel. *PLoS ONE* **5**, e12943.
Babcock, D. T., Brock, A. R., Fish, G. S., Wang, Y., Perrin, L., Krasnow, M. A. and Galko, M. J. (2008). Circulating blood cells function as a surveillance system for damaged tissue in *Drosophila* larvae. *Proc. Natl. Acad. Sci. USA* **105**, 10017-10022.
Boppana, S. and Hillyer, J. F. (2014). Hemolymph circulation in insect sensory appendages: functional mechanics of antennal accessory pulsatile organs (auxiliary hearts) in the mosquito *Anopheles gambiae*. *J. Exp. Biol.* **217**, 3006-3014.
Chapman, R. F., Douglas, A. E. and Siva-Jothy, M. T. (2013). Circulatory system, blood, and the immune system. In *The Insects: Structure and Function* (ed. S. J. Simpson and A. E. Douglas), pp. 107-131. Cambridge: Cambridge University Press.
Chen, W. and Hillyer, J. F. (2013). FlyNap (triethylamine) increases the heart rate of mosquitoes and eliminates the cardioacceleratory effect of the neuropeptide CCAP. *PLoS ONE* **8**, e70414.
Curtis, N. J., Ringo, J. M. and Dowse, H. B. (1999). Morphology of the pupal heart, adult heart, and associated tissues in the fruit fly, *Drosophila melanogaster*. *J. Morphol.* **240**, 225-235.
Dasari, S. and Cooper, R. L. (2006). Direct influence of serotonin on the larval heart of *Drosophila melanogaster*. *J. Comp. Physiol. B* **176**, 349-357.
Davis, N. T., Dulcis, D. and Hildebrand, J. G. (2001). Innervation of the heart and aorta of *Manduca sexta*. *J. Comp. Neurol.* **440**, 245-260.
Dulcis, D. and Levine, R. B. (2003). Innervation of the heart of the adult fruit fly, *Drosophila melanogaster*. *J. Comp. Neurol.* **465**, 560-578.
Dulcis, D. and Levine, R. B. (2004). Remodeling of a larval skeletal muscle motoneuron to drive the posterior cardiac pacemaker in the adult moth, *Manduca sexta*. *J. Comp. Neurol.* **478**, 126-142.
Dulcis, D. and Levine, R. B. (2005). Glutamatergic innervation of the heart initiates retrograde contractions in adult *Drosophila melanogaster*. *J. Neurosci.* **25**, 271-280.
Dulcis, D., Davis, N. T. and Hildebrand, J. G. (2001). Neuronal control of heart reversal in the hawkmoth *Manduca sexta*. *J. Comp. Physiol. A* **187**, 837-849.
Dulcis, D., Levine, R. B. and Ewer, J. (2005). Role of the neuropeptide CCAP in *Drosophila* cardiac function. *J. Neurobiol.* **64**, 259-274.
Estévez-Lao, T. Y., Boyce, D. S., Honegger, H. W. and Hillyer, J. F. (2013). Cardioacceleratory function of the neurohormone CCAP in the mosquito *Anopheles gambiae*. *J. Exp. Biol.* **216**, 601-613.
Favia, G., Ricci, I., Damiani, C., Raddadi, N., Crotti, E., Marzorati, M., Rizzi, A., Urso, R., Brusetti, L., Borin, S. et al. (2007). Bacteria of the genus Asaia stably associate with *Anopheles stephensi*, an Asian malarial mosquito vector. *Proc. Natl. Acad. Sci. USA* **104**, 9047-9051.
Fillinger, U. and Lindsay, S. W. (2011). Larval source management for malaria control in Africa: myths and reality. *Malar. J.* **10**, 353.
Gerould, J. H. (1924). Periodic reversal of heart-beat in a chrysalis. *Science* **60**, 570-572.
Gerould, J. H. (1933). Orders of insects with heart-beat reversal. *Biol. Bull.* **64**, 424-431.
Glenn, J. D., King, J. G. and Hillyer, J. F. (2010). Structural mechanics of the mosquito heart and its function in bidirectional hemolymph transport. *J. Exp. Biol.* **213**, 541-550.
Harrison, J. F., Woods, H. A. and Roberts, S. P. (2012). *Ecological and Environmental Physiology of Insects*. New York, NY: Oxford University Press.
Hillyer, J. F., Barreau, C. and Vernick, K. D. (2007). Efficiency of salivary gland invasion by malaria sporozoites is controlled by rapid sporozoite destruction in the mosquito haemocoel. *Int. J. Parasitol.* **37**, 673-681.
Hillyer, J. F., Estévez-Lao, T. Y., Funkhouser, L. J. and Aluoch, V. A. (2012). *Anopheles gambiae* corazonin: gene structure, expression and effect on mosquito heart physiology. *Insect Mol. Biol.* **21**, 343-355.
Hillyer, J. F., Estévez-Lao, T. Y. and de la Parte, L. E. (2014). Myotropic effects of FMRFamide containing peptides on the heart of the mosquito *Anopheles gambiae*. *Gen. Comp. Endocrinol.* **202**, 15-25.
Jones, J. C. (1954). The heart and associated tissues of *Anopheles quadrimaculatus* Say (Diptera: Culicidae). *J. Morphol.* **94**, 71-123.
Jones, J. C. (1977). *The Circulatory System of Insects*. Springfield, IL: Charles C. Thomas.
King, J. G. and Hillyer, J. F. (2012). Infection-induced interaction between the mosquito circulatory and immune systems. *PLoS Pathog.* **8**, e1003058.
King, J. G. and Hillyer, J. F. (2013). Spatial and temporal in vivo analysis of circulating and sessile immune cells in mosquitoes: hemocyte mitosis following infection. *BMC Biol.* **11**, 55.
Klowden, A. J. (2013). Circulatory systems. In *Physiological Systems in Insects*, pp. 365-413. Boston, MA: Academic Press.
Kuwasawa, K., Ai, H. and Matsushita, T. (1999). Cardiac reflexes and their neural pathways in lepidopterous insects. *Comp. Biochem. Physiol.* **124**, 581-586.
Lehmacher, C., Abeln, B. and Paululat, A. (2012). The ultrastructure of *Drosophila* heart cells. *Arthropod Struct. Dev.* **41**, 459-474.
Leódido, A. C., Ramalho-Ortigão, M. and Martins, G. F. (2013). The ultrastructure of the *Aedes aegypti* heart. *Arthropod Struct. Dev.* **42**, 539-550.
Locke, M. (1997). Caterpillars have evolved lungs for hemocyte gas exchange. *J. Insect Physiol.* **44**, 1-20.
Martins, G. F., Ramalho-Ortigão, J. M. and Pimenta, P. F. P. (2011). Morphological features of the heart of six mosquito species as revealed by scanning electron microscopy. *Int. J. Trop. Insect Sci.* **31**, 98-102.
Matsushita, T., Kuwasawa, K., Uchimura, K., Ai, H. and Kurokawa, M. (2002). Biogenic amines evoke heartbeat reversal in larvae of the sweet potato hornworm, *Agrius convolvuli*. *Comp. Biochem. Physiol.* **133A**, 625-636.
Miller, T. A. (1985). Structure and physiology of the circulatory system. In *Comprehensive Insect Physiology, Biochemistry and Pharmacology* (ed. G. A. Kirkut and L. I. Gilbert), pp. 289-333. Oxford: Pergamon.
Miller, T. A. (1997). Control of circulation in insects. *Gen. Pharmacol.* **29**, 23-38.
Molina, M. R. and Cripps, R. M. (2001). Ostia, the inflow tracts of the *Drosophila* heart, develop from a genetically distinct subset of cardial cells. *Mech. Dev.* **109**, 51-59.
Nation, J. L. (2008). Circulatory system. In *Insect Physiology and Biochemistry*, pp. 339-365. Boca Raton, FL: CRC Press.
Otieno-Ayayo, Z. N., Zaritsky, A., Wirth, M. C., Manasherob, R., Khasdan, V., Cahan, R. and Ben-Dov, E. (2008). Variations in the mosquito larvicidal activities of toxins from *Bacillus thuringiensis* ssp. *israelensis*. *Environ. Microbiol.* **10**, 2191-2199.
Paily, K. P., Geetha, I., Kumar, B. A. and Balaraman, K. (2012). *Bacillus sphaericus* in the adults of *Culex quinquefasciatus* mosquitoes emerged from treated larvae and its effect on development of the filarial parasite, *Wuchereria bancrofti*. *Parasitol. Res.* **110**, 2229-2235.
Piazza, N. and Wessells, R. J. (2011). *Drosophila* models of cardiac disease. *Prog. Mol. Biol. Transl. Sci.* **100**, 155-210.
Rao, A., Henderson, R. E. and Bradleigh Vinson, S. (2009). The probable significance of tracheal tufts in the 8th abdominal segment of *Heliothis virescens* (F.) on the development of its parasitoid, *Toxoneuron nigriceps* (Viereck). *J. Insect Physiol.* **55**, 769-773.
Sláma, K. and Farkas, R. (2005). Heartbeat patterns during the postembryonic development of *Drosophila melanogaster*. *J. Insect Physiol.* **51**, 489-503.
Smits, A. W., Burggren, W. W. and Oliveras, D. (2000). Developmental changes in in vivo cardiac performance in the moth *Manduca sexta*. *J. Exp. Biol.* **203**, 369-378.
Uchimura, K., Ai, H., Kuwasawa, K., Matsushita, T. and Kurokawa, M. (2006). Excitatory neural control of posterograde heartbeat by the frontal ganglion in the last instar larva of a lepidopteran, *Bombyx mori*. *J. Comp. Physiol. A* **192**, 175-185.

Wasserthal, L. T. (1980). Oscillating haemolymph 'circulation' in the butterfly *Papilio machaon* L. revealed by contact thermography and photocell measurements. *J. Comp. Physiol.* **139**, 145-163.
Wasserthal, L. T. (1981). Oscillating haemolymph 'circulation' and discontinuous tracheal ventilation in the giant silk moth *Attacus atlas* L. *J. Comp. Physiol.* **145**, 1-15.
Wasserthal, L. T. (1999). Functional morphology of the heart and of a new cephalic pulsatile organ in the blowfly *Calliphora vicina* (Diptera: Calliphoridae) and their roles in hemolymph transport and tracheal ventilation. *Int. J. Insect Morphol. Embryol.* **28**, 111-129.
Wasserthal, L. T. (2003). Circulation and thermoregulation. In *Lepidoptera, Moths and Butterflies: Morphology, Physiology, and Development*, Vol. 2 (ed. N. Kristensen), pp. 205-228. New York, NY: Walter De Gruyter.
Wasserthal, L. T. (2007). *Drosophila* flies combine periodic heartbeat reversal with a circulation in the anterior body mediated by a newly discovered anterior pair of ostial valves and 'venous' channels. *J. Exp. Biol.* **210**, 3707-3719.
Wasserthal, L. T. (2012). Influence of periodic heartbeat reversal and abdominal movements on hemocoelic and tracheal pressure in resting blowflies *Calliphora vicina*. *J. Exp. Biol.* **215**, 362-373.

Movie 1. Heart contractions of a mosquito larva and adult.

Movie 2. Hemolymph flow through the heart of a mosquito larva and adult.

Movie 3. Hemolymph flow across the ventral hemocoel of a mosquito larva.

Movie 4. 3D rendering of a segment of the heart of a mosquito larva.

Movie 5. Hemolymph entering the heart of a mosquito larva through the posterior incurrent openings.

Movie 6. Hemolymph exiting the aorta of a mosquito larva at the base of the head.